To cite this article: Yu Y L, Su R B, Feng X, et al. Tracking control of backstepping adaptive path of unmanned surface vessels based on surge-varying LOS[J/OL]. Chinese Journal of Ship Research, 2019, 14(3). http://www.ship-research.com/CN/Y2019/V14/I3/163.

DOI:10.19693/j.issn.1673-3185.01377

Tracking control of backstepping adaptive path of unmanned surface vessels based on surge-varying LOS

Yu Yalei[1], *Su Rongbin*[1], *Feng Xu*[1], *Guo Chen*[*2]

1 Navigation College, Dalian Maritime University, Dalian 116026, China

2 Marine Electrical Engineering College, Dalian Maritime University, Dalian 116026, China

Abstract: [**Objectives**] To solve lumped uncertainties of Unmanned Surface Vessels (USV) caused by system modeling errors and parameter perturbations, and path tracking problem of the model including non-zero non-diagonal terms and controller input saturation, [**Methods**] a tracking control method of backstepping adaptive path of USV based on surge-varying Line-of-Sight (LOS) is proposed. First of all, a coordinate transformation is introduced to transform system model into skew-symmetric form. The controlled system is divided into two subsystems, guidance subsystem and control subsystem, respectively. In the guidance subsystem, the surge-varying LOS algorithm is developed to make guidance law of longitudinal speed positively correlated to transverse tracking error and ensure USV can effectively go towards and keep on the expected path; In the control subsystem, the lumped uncertainties of system are compensated by constructing backstepping adaptive algorithm. Simultaneously, the auxiliary system is introduced to deal with the problem caused by saturation of system control input. [**Results**] The guidance-control closed-loop system is proved to be uniformly ultimately bounded by using Lyapunov stability theories. [**Conclusions**] Simulation results verify the effectiveness and robustness of the proposed method. It has certain reference value for tracking control of backstepping adaptive path of unmanned surface vessels.

Key words: Unmanned Surface Vessels (USV); path tracking; Line-of-Sight (LOS); input saturations; adaptive control

CLC number: U664.82

0 Introduction

Over the past decade, the unmanned surface vessels (USV) have been extensively applied in search and rescue, scientific research, exploration and commercial fields [1-5]. The main research issues of USV motion control include flight path tracking, formation control, and stabilization control, among which the flight path tracking can be divided into trajectory tracking and path tracking [6]. Trajectory tracking means that USV can reach the designated position at the specified time. While the path tracking only needs to complete geometric position tracking and does not depend on the time information. In fact, when a vessel is sailing on the ocean, it is generally not required to arrive at the appointed place within a specified time, but sails along the planned route. Therefore, path tracking is of great significance to navigation practice [7]. Wang et al. [8-14] made many achievements in the research of path tracking guidance based on line-of-sight (LOS)[14-15]. The improvement of LOS is mainly carried out from two aspects: the first is from the geometrical aspect without considering the influence of drift angle on the guidance

Received: 2018-08-15

Supported by: National Natural Science Foundation of China (51879027, 51579024, 6137114, 51809028); Fundamental Research Funds for the Central Universities (Dalian Maritime University 3132016311, 3132018154)

Author(s): Yu Yalei, male, born in 1992, master degree candidate. Research interests: ship motion control and nonlinear control. E-mail: yuyalei89@gmail.com

Guo Chen, male, born in 1956, Ph.D., professor. Research interests: intelligent control and ship automation system. E-mail: dmuguoc@126.com

***Corresponding author:** Guo Chen

course, and the second is from the aspect of how to obtain a more accurate drift angle with the consideration of the influence of the drift angle on guidance course[8, 10, 13]. The LOS with an improved drift angle can be divided into three categories, namely LOSs applicable to small drift angle (less than 5°) and large drift angle, and LOS separately studying the drift angles of ocean current and transverse motion[8]. Shi et al. [16] solved the problem of vessel path tracking control with backstepping. In addition, backstepping can also be combined with other methods to solve the problems of parameter perturbation of system model, modeling error and model-free [3,4]. Do et al. [17] adopted the neural network based on the backstepping and adaptive method to solve the problem of stable tracking. In order to achieve more complex control objectives and adapt to more complex external environment, many scholars have achieved certain results using intelligent control methods, such as reinforcement learning, and sliding mode [18-20]. However, control inputs are inevitably affected by the actuator saturation. The design of the auxiliary system is a commonly adopted method to deal with the saturation of control input, mainly including direct restriction of control input and indirect restriction of system state quantity, so as to restrict the actual amplitude of control input [1, 21-23]. In the above references, most models of USV are assumed to be diagonal, because the non-zero non-diagonal inertia matrix will make the yaw moment act not only in the direction of yawing but also in transverse motion, which increases the difficulty of controller design and destroys the cascade structure of the control system. The key to solving the problem is to eliminate the control moment acting in the transverse motion. The methods to this problem mainly include methods of system state transformation, control output transformation, and selection of appropriate coordinate origin of vessel system [17,24-25].

Inspired by the above methods, the influence of drift angle and transverse tracking error on guidance course is considered to design the guidance law of surge-varying LOS and the backstepping adaptive control law with the auxiliary system. Firstly, the coordinate transformation method is introduced to transfer the non-zero non-diagonal of inertia matrix into a skew-symmetric form, so as to simplify the design of the system controller. Then, the guidance law of surge-varying LOS is designed in the guidance subsystem to ensure that USV can effectively go towards and keep on the expected path. In the control subsystem, the backstepping adaptive and auxiliary system algorithm are respectively designed to deal with the lumped uncertainties and problems of control input saturation. Next, the guidance-control closed-loop system is proved to be uniformly bounded using Lyapunov stability theories. Finally, the effectiveness and robustness of the proposed method are proved by simulation experiments.

1 Mathematical model and hypothesis

1.1 Mathematical model

The mathematical model of USV in the horizontal plane can be described as [5]

$$\begin{cases} \dot{\boldsymbol{\eta}} = \boldsymbol{J}(\psi)\boldsymbol{v} \\ \boldsymbol{M}\dot{\boldsymbol{v}} = -\boldsymbol{C}(\boldsymbol{v})\boldsymbol{v} - \boldsymbol{D}(\boldsymbol{v})\boldsymbol{v} + \boldsymbol{\tau} + \boldsymbol{b} \end{cases} \tag{1}$$

where $\boldsymbol{\eta}$ is the vessel position and course vector; $\boldsymbol{J}(\psi)$ is the rotation matrix between the geodetic coordinate system and the coordinate system of hull; $\boldsymbol{v}$ is the velocity vector; $\boldsymbol{M}$ is the inertia coefficient matrix; $\boldsymbol{C}$ is the Coriolis centripetal force matrix; $\boldsymbol{D}$ is the damping coefficient matrix; $\boldsymbol{\tau}$ is the control input vector; and $\boldsymbol{b}$ is the external interference vector. Among them,

$$\boldsymbol{\eta} = \begin{bmatrix} x \\ y \\ \psi \end{bmatrix}, \quad \boldsymbol{v} = \begin{bmatrix} u \\ v \\ r \end{bmatrix}, \quad \boldsymbol{\tau} = \begin{bmatrix} \tau_u \\ 0 \\ \tau_r \end{bmatrix}, \quad \boldsymbol{b} = \begin{bmatrix} b_1 \\ b_2 \\ b_3 \end{bmatrix}$$

$$\boldsymbol{M} = \begin{bmatrix} m_{11} & 0 & 0 \\ 0 & m_{22} & m_{23} \\ 0 & m_{32} & m_{33} \end{bmatrix}, \quad \boldsymbol{D} = \begin{bmatrix} d_{11} & 0 & 0 \\ 0 & d_{22} & d_{23} \\ 0 & d_{32} & d_{33} \end{bmatrix}$$

$$\boldsymbol{J}(\psi) = \begin{bmatrix} \cos\psi & -\sin\psi & 0 \\ \sin\psi & \cos\psi & 0 \\ 0 & 0 & 1 \end{bmatrix}$$

$$\boldsymbol{C}(\boldsymbol{v}) = \begin{bmatrix} 0 & 0 & -m_{22}v - m_{23}r \\ 0 & 0 & m_{11}u \\ m_{22}v + m_{23}r & -m_{11}u & 0 \end{bmatrix}$$

where (x, y, ψ) are respectively the longitudinal position, transverse position and yawing angle in the geodetic coordinate system; (u, v, r) are respectively the longitudinal, transverse and yawing velocity in the coordinate system of hull; τ_u and τ_r represent control force and control moment in the coordinate system of hull. b_1, b_2, b_3 are external disturbances caused by external wind, wave, and current; m_{11}, m_{22}, m_{33}, m_{23} and m_{32} are inertial masses; d_{11}, d_{22}, d_{33}, d_{23} and d_{32} are hydrodynamic derivatives.

In order to transform the dynamic state of USV into the "skew-symmetric" form, the following coordinate transformation is introduced [24]

$$\bar{x}=x+\varepsilon\cos\psi,\quad \bar{y}=y+\varepsilon\sin\psi,\quad \bar{v}=v+\varepsilon r \tag{2}$$

where $\varepsilon=m_{23}/m_{22}$. Replacing $(\bar{x},\bar{y},\psi)$ with (x,y,ψ) and substituting Eq. (2) into Eq. (1), we can obtain

$$\begin{cases}\dot{\bar{x}}=u\cos\psi-\bar{v}\sin\psi\\ \dot{\bar{y}}=u\sin\psi+\bar{v}\cos\psi\\ \dot{\psi}=r\\ \dot{u}=\boldsymbol{f}_u^{\mathrm{T}}\boldsymbol{\chi}_u(\boldsymbol{v})+\boldsymbol{g}_u^{\mathrm{T}}\boldsymbol{\chi}(\boldsymbol{b})+h_u\tau_u\\ \dot{\bar{v}}=\boldsymbol{f}_{\bar{v}}^{\mathrm{T}}\boldsymbol{\chi}_{\bar{v}}(\boldsymbol{v})+\boldsymbol{g}_{\bar{v}}^{\mathrm{T}}\boldsymbol{\chi}(\boldsymbol{b})\\ \dot{r}=\boldsymbol{f}_r^{\mathrm{T}}\boldsymbol{\chi}_r(\boldsymbol{v})+\boldsymbol{g}_r^{\mathrm{T}}\boldsymbol{\chi}(\boldsymbol{b})+h_r\tau_r\end{cases} \tag{3}$$

where

$$\boldsymbol{f}_u=\begin{bmatrix}\frac{m_{22}}{m_{11}} & -\frac{d_{11}}{m_{11}} & 0\end{bmatrix}^{\mathrm{T}}$$

$$\boldsymbol{g}_u=\begin{bmatrix}\frac{1}{m_{11}} & 0 & 0\end{bmatrix}^{\mathrm{T}}$$

$$\boldsymbol{\chi}_u(\boldsymbol{v})=\begin{bmatrix}\bar{v}r & -u & r\end{bmatrix}^{\mathrm{T}}$$

$$\boldsymbol{\chi}(\boldsymbol{b})=\begin{bmatrix}b_1 & b_2 & b_3\end{bmatrix}^{\mathrm{T}}$$

$$h_u=\frac{1}{m_{11}}$$

$$\boldsymbol{f}_{\bar{v}}=\begin{bmatrix}\frac{m_{11}}{m_{22}} & \frac{d_{22}}{m_{22}} & \frac{d_{22}m_{23}-d_{32}m_{22}}{m_{22}^2}\end{bmatrix}^{\mathrm{T}}$$

$$\boldsymbol{\chi}_{\bar{v}}(\boldsymbol{v})=\begin{bmatrix}-ur & -\bar{v} & r\end{bmatrix}^{\mathrm{T}}$$

$$\boldsymbol{g}_{\bar{v}}=\begin{bmatrix}0 & \frac{1}{m_{22}} & 0\end{bmatrix}$$

$$\boldsymbol{\chi}_r(\boldsymbol{v})=\begin{bmatrix}u\bar{v} & \bar{v} & -r\end{bmatrix}^{\mathrm{T}}$$

$$h_r=\frac{m_{22}}{m_{22}m_{33}-m_{23}^2}$$

$$\boldsymbol{g}_r=\begin{bmatrix}0 & -\frac{m_{23}}{m_{22}m_{33}-m_{23}^2} & \frac{m_{22}}{m_{22}m_{33}-m_{23}^2}\end{bmatrix}^{\mathrm{T}}$$

$$\boldsymbol{f}_r=\begin{bmatrix}\frac{m_{11}m_{22}-m_{22}^2}{m_{22}m_{33}-m_{23}^2} & \frac{d_{22}m_{23}-d_{32}m_{22}}{m_{22}m_{33}-m_{23}^2}\\ \frac{-d_{32}m_{23}m_{22}-d_{23}m_{23}m_{22}+d_{33}m_{22}^2-d_{22}m_{23}^2}{m_{22}\left(m_{22}m_{33}-m_{23}^2\right)}\end{bmatrix}^{\mathrm{T}}$$

Control laws: τ_u and τ_r are designed to set the control objective as making the position of USV (x,y) converges to the parameterized path set $\eta_{\mathrm{p}}(\theta):=\left(x_{\mathrm{p}}(\theta),y_{\mathrm{p}}(\theta)\right)\in\mathbb{R}^q$, $q\geqslant 1$, so as to make USV track the desired path. When $t\to\infty$, the forward and transverse tracking errors meet $x_{\mathrm{e}}\to 0$ and $y_{\mathrm{e}}\to 0$.

1.2 Hypothesis

This paper is based on the following hypothesis:

1) The USV is symmetrical about the xz plane, and the heaving, pitching and rolling motions are very small, which can be ignored. The center of buoyancy of USV coincides with the center of gravity. In the coordinate system of hull, the coordinate origin is on the center line of USV, which is a rigid body with uniform mass distribution.

2) The parameter perturbation is slow time-varying and satisfies $|F_u|<F_{u\max}<\infty$ and $|F_r|<F_{r\max}<\infty$.

3) The transverse velocity v is passively bounded and stable [4] and satisfies $|v|\leqslant v_{\max}<\infty$.

Based on assumption 3 and coordinate transformation, it can be obtained that the longitudinal velocity after transformation is bounded and satisfies $|\bar{v}|\leqslant v_{\max}+\varepsilon|r|_{\max}<\infty$.

4) The actual control input $\tau_i(i=u,r)$ is bounded and satisfies $|\tau_i|\leqslant\tau_{i\max}<\infty$. Thus, there is

$$\tau_i=\begin{cases}\tau_{i\max}, & \tau_i>\tau_{i\max}\\ \tau_{i0}, & -\tau_{i\max}\leqslant\tau_{i0}\leqslant\tau_{i\max}\\ -\tau_{i\max}, & \tau_{i0}<-\tau_{i\max}\end{cases} \tag{4}$$

2 Dynamic path error

For the movement of USV in the path tracking process, its forward and transverse tracking error variable $(x_{\mathrm{e}},y_{\mathrm{e}})$ is defined by the connection line between the normal line at point $\left(x_{\mathrm{p}}(\theta),y_{\mathrm{p}}(\theta)\right)$ on the parameterized path and point (x,y), as shown in Fig. 1. And X_{p} and Y_{p} are respectively the horizontal and vertical coordinates of the tangent system.

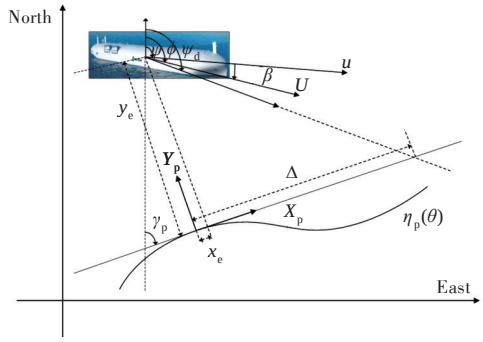

Fig.1 Geometrical illustration based on LOS guidance

To effectively track the desired path, the path error variable in the coordinate system of hull is converted to the tangent coordinate system of the desired path:

$$\begin{bmatrix}x_{\mathrm{e}}\\ y_{\mathrm{e}}\end{bmatrix}=\boldsymbol{R}\left(\gamma_{\mathrm{p}}\right)^{\mathrm{T}}\begin{bmatrix}\bar{x}-x_f\\ \bar{y}-y_f\end{bmatrix} \tag{5}$$

where $x_f=x_{\mathrm{p}}+\frac{m_{23}}{m_{22}}\cos\gamma_{\mathrm{p}};y_f=y_{\mathrm{p}}+\frac{m_{23}}{m_{22}}\sin\gamma_{\mathrm{p}}$; $\boldsymbol{R}\left(\gamma_{\mathrm{p}}\right)$ is the rotation transformation matrix,

$$\boldsymbol{R}\left(\gamma_{\mathrm{p}}\right)=\begin{bmatrix}\cos\gamma_{\mathrm{p}} & -\sin\gamma_{\mathrm{p}}\\ \sin\gamma_{\mathrm{p}} & \cos\gamma_{\mathrm{p}}\end{bmatrix} \tag{6}$$

and γ_{p} is the expected path tangent angle and its ex-

pression is

$$\gamma_{\mathrm{p}}=\operatorname{atan2}\left(y_{\mathrm{p}}^{'}(\theta),x_{\mathrm{p}}^{'}(\theta)\right):=[-\pi,\pi] \tag{7}$$

Taking the derivative of the forward error x_{e} with respect to time, we can obtain

$$\dot{x}_{\mathrm{e}}=\left(\dot{\bar{x}}-\dot{x}_{\mathrm{p}}+\dot{\gamma}_{\mathrm{p}}\frac{m_{23}}{m_{22}}\sin\gamma_{\mathrm{p}}\right)\cos\gamma_{\mathrm{p}}-\left(\bar{x}-x_f\right)\dot{\gamma}_{\mathrm{p}}\sin\gamma_{\mathrm{p}}+$$

$$\left(\dot{\bar{y}}-\dot{y}_{\mathrm{p}}-\dot{\gamma}_{\mathrm{p}}\frac{m_{23}}{m_{22}}\cos\gamma_{\mathrm{p}}\right)\sin\gamma_{\mathrm{p}}+\left(\bar{y}-y_f\right)\dot{\gamma}_{\mathrm{p}}\cos\gamma_{\mathrm{p}}=$$

$$\underbrace{\dot{\bar{x}}\cos\gamma_{\mathrm{p}}+\dot{\bar{y}}\sin\gamma_{\mathrm{p}}}_{m_1}-\dot{\gamma}_{\mathrm{p}}\underbrace{\left(\left(\bar{y}-y_f\right)\cos\gamma_{\mathrm{p}}-\left(\bar{x}-x_f\right)\sin\gamma_{\mathrm{p}}\right)}_{\text{along-tracking error }y_{\mathrm{e}}}-$$

$$\underbrace{\dot{x}_{\mathrm{p}}(\theta)\cos\gamma_{\mathrm{p}}-\dot{y}_{\mathrm{p}}(\theta)\sin\gamma_{\mathrm{p}}}_{m_2} \tag{8}$$

where $\dot{x}_f=\dot{x}_{\mathrm{p}}-\dot{\gamma}_{\mathrm{p}}\frac{m_{23}}{m_{22}}\sin\gamma_{\mathrm{p}}$; $\dot{y}_f=\dot{y}_{\mathrm{p}}+\dot{\gamma}_{\mathrm{p}}\frac{m_{23}}{m_{22}}\cos\gamma_{\mathrm{p}}$; $\dot{x}_{\mathrm{p}}=\dot{\theta}x_{\mathrm{p}}^{'}(\theta)$; $\dot{y}_{\mathrm{p}}=\dot{\theta}y_{\mathrm{p}}^{'}(\theta)$. And then m_1 is expressed in amplitude and phase form

$$m_1=\sqrt{u^2+\bar{v}^2}\cos\left(\psi-\gamma_{\mathrm{p}}+\beta\right) \tag{9}$$

where β is the drift angle between the course angle and the heading angle, namely $\beta=\phi-\psi=\operatorname{atan2}(\bar{v},u)$, and it is the four-quadrant form of the arctangent function $\arctan\left(\frac{\bar{v}}{u}\right)\in\left[\frac{\pi}{2},-\frac{\pi}{2}\right]$. $U(u,\bar{v}):=\sqrt{u^2+\bar{v}^2}$.

Moreover, m_2 of Eq. (8) can be rewritten as

$$m_2=\dot{x}_{\mathrm{p}}(\theta)\cos\gamma_{\mathrm{p}}-\dot{y}_{\mathrm{p}}(\theta)\sin\gamma_{\mathrm{p}}=$$

$$\dot{\theta}\sqrt{y_{\mathrm{p}}^{'2}(\theta)+x_{\mathrm{p}}^{'2}(\theta)}\cos\left(\gamma_{\mathrm{p}}+\phi\right) \tag{10}$$

where $\phi=\operatorname{atan2}\left(-y_{\mathrm{p}}^{'}(\theta),x_{\mathrm{p}}^{'}(\theta)\right)=-\gamma_{\mathrm{p}}$; $y_{\mathrm{p}}^{'}(\theta)$ is the derivative of $y_{\mathrm{p}}(\theta)$ with respect to θ.

According to Eq. (10), there is

$$u_{\mathrm{tot}}:=m_2=\dot{\theta}\sqrt{y_{\mathrm{p}}^{'2}(\theta)+x_{\mathrm{p}}^{'2}(\theta)} \tag{11}$$

where u_{tot} is the velocity of the virtual reference point on the expected path. Thus, there is

$$\dot{x}_{\mathrm{e}}=\sqrt{u^2+\bar{v}^2}\cos\left(\psi-\gamma_{\mathrm{p}}+\beta\right)+y_{\mathrm{e}}\dot{\gamma}_{\mathrm{p}}-u_{\mathrm{tot}} \tag{12}$$

Similarly, the derivative of the transverse position error is

$$\dot{y}_{\mathrm{e}}=\sqrt{u^2+\bar{v}^2}\sin\left(\psi-\gamma_{\mathrm{p}}+\beta\right)-x_{\mathrm{e}}\dot{\gamma}_{\mathrm{p}} \tag{13}$$

Since the drift angle β is very small and generally less than 5° [13], the non-zero time-varying drift angle in static water can be ignored. Therefore, there is $\beta\approx\sin\beta$, and then the dynamic position error can be simplified to

$$\begin{cases}\dot{x}_{\mathrm{e}}=\sqrt{u^2+\bar{v}^2}\cos\left(\psi-\gamma_{\mathrm{p}}+\sin\beta\right)+y_{\mathrm{e}}\dot{\gamma}_{\mathrm{p}}-u_{\mathrm{tot}}\\ \dot{y}_{\mathrm{e}}=\sqrt{u^2+\bar{v}^2}\sin\left(\psi-\gamma_{\mathrm{p}}+\sin\beta\right)-x_{\mathrm{e}}\dot{\gamma}_{\mathrm{p}}\end{cases} \tag{14}$$

3 Guidance-control design

The guidance-control closed-loop design consists of two parts, namely the guidance subsystem and the control subsystem. In the first part, the law of surge-varying LOS is developed to ensure that USV can effectively go towards and keep on the expected path. In the control subsystem, considering the lumped uncertainties and control input saturation, the backstepping adaptive system and the auxiliary system are employed to design the law of longitudinal and yawing direction control τ_u and τ_r.

3.1 Guidance law of surge-varying LOS design

To design the guidance law of surge-varying LOS, the guidance law of longitudinal velocity is firstly designed as [3]

$$u_{\mathrm{d}}=k\sqrt{\Delta^2+y_{\mathrm{e}}^2} \tag{15}$$

where Δ is the forward distance of LOS guidance, $\{k,\Delta\}>0$, and k is a positive control parameter.

Restricted by the characteristics of vessel actuator, the thrust produced by the propeller and the yaw moment produced by the rudder cannot be infinite, and thus the maximum velocity of USV is bounded, namely $0<k\Delta<u_{\mathrm{d}}<u_{\max}<\infty$. Therefore, when the initial transverse velocity is too high, the saturation limit on the guidance law of longitudinal velocity is needed, namely

$$u_{\mathrm{d}}=\operatorname{sat}\left(u_{\mathrm{d}}\right)=\begin{cases}u_{\max}, & u_{\mathrm{d}}>u_{\max}\\ u_{\mathrm{d}}, & k\Delta<u_{\mathrm{d}}<u_{\max}\\ k\Delta, & u_{\mathrm{d}}<k\Delta\end{cases} \tag{16}$$

The expected design course is

$$\psi_{\mathrm{d}}=\gamma_{\mathrm{p}}(\theta)+\arcsin\left(\frac{-\Delta y_{\mathrm{e}}}{\sqrt{1+\left(\Delta y_{\mathrm{e}}\right)^2}}\right)-\sin\beta \tag{17}$$

In fact, the expected course angle ψ_{d} can be accurately tracked by the practical course ψ. Therefore, we can obtain

$$\psi-\gamma_{\mathrm{p}}(\theta)\simeq\psi_{\mathrm{d}}-\gamma_{\mathrm{p}}(\theta)=$$

$$\arcsin\left(-\frac{\Delta y_{\mathrm{e}}}{\sqrt{1+\left(0.1y_{\mathrm{e}}\right)^2}}\right)-\sin\beta \tag{18}$$

In the first equation of Eq. (14), u_{tot} can be regarded as a virtual control law to stabilize the forward position errors. Therefore, the design of it is

$$u_{\mathrm{tot}}=k_1x_{\mathrm{e}}+U\cos\left(\psi-\gamma_{\mathrm{p}}+\sin\beta\right) \tag{19}$$

where k_1 is a positive design parameter.

Substituting Eq. (17) and Eq. (19) into Eq. (14), there is

$$\begin{cases}\dot{x}_{\mathrm{e}}=-k_1x_{\mathrm{e}}+y_{\mathrm{e}}\dot{\gamma}_{\mathrm{p}}\\ \dot{y}_{\mathrm{e}}=-U\dfrac{\Delta y_{\mathrm{e}}}{\sqrt{1+\left(\Delta y_{\mathrm{e}}\right)^2}}-x_{\mathrm{e}}\dot{\gamma}_{\mathrm{p}}\end{cases} \tag{20}$$

Lyapunov function is constructed as

$$V_1 = \frac{1}{2}x_e^2 + \frac{1}{2}y_e^2 \tag{21}$$

Taking the derivative of V_1 with respect to time and combining with Eq. (20), we can obtain

$$\dot{V}_1 = -k_1 x_e^2 - k_y y_e^2 \tag{22}$$

where $0 < k_y := \dfrac{\Delta U}{\sqrt{1+(\Delta y_e)^2}} < \infty$. Since $0 < U_{\min} < U < U_{\max}$, we can see that $\dot{V}_1 \leqslant 0$.

3.2 Controller design

In this section, it is assumed that the external disturbance to the USV can be ignored. In this case, Eq. (3) can be rewritten as

$$\begin{cases} \dot{u} = \left(\boldsymbol{f}_u^{\mathrm{T}} + \Delta\boldsymbol{f}_u^{\mathrm{T}}\right)\boldsymbol{\chi}_u(\boldsymbol{v}) + \left(h_u + \Delta h_u\right)\tau_u = \\ \quad \boldsymbol{f}_u^{\mathrm{T}}\boldsymbol{\chi}_u(\boldsymbol{v}) + h_u\tau_u + F_u \\ \dot{\bar{v}} = \left(\boldsymbol{f}_{\bar{v}}^{\mathrm{T}} + \Delta\boldsymbol{f}_{\bar{v}}^{\mathrm{T}}\right)\boldsymbol{\chi}_{\bar{v}}(\boldsymbol{v}) = \boldsymbol{f}_{\bar{v}}^{\mathrm{T}}\boldsymbol{\chi}_{\bar{v}}(\boldsymbol{v}) + F_v \\ \dot{r} = \left(\boldsymbol{f}_r^{\mathrm{T}} + \Delta\boldsymbol{f}_{\bar{v}}^{\mathrm{T}}\right)\boldsymbol{\chi}_r(\boldsymbol{v}) + \left(h_r + \Delta h_r\right)\tau_r = \\ \quad \boldsymbol{f}_r^{\mathrm{T}}\boldsymbol{\chi}_r(\boldsymbol{v}) + h_r\tau_r + F_r \end{cases} \tag{23}$$

Variable errors ψ_e, r_e and u_e are defined as

$$\psi_e := \psi - \psi_d, \quad r_e := r - r_d, \quad u_e := u - u_d \tag{24}$$

where $r_d = -k_\psi\psi_e + \dot{\psi}_d$ and k_ψ is the positive design parameter.

Considering the actuator saturation, the nominal law of longitudinal control and the law of yaw control are designed as

$$\tau_{u0} = -\left(\lambda_u u_e + \boldsymbol{f}_u^{\mathrm{T}}\boldsymbol{\chi}_u(\boldsymbol{v}) - \dot{u}_d + \hat{F}_u - k_{u0}\chi_u\right) \tag{25}$$

$$\tau_{r0} = -\left(\lambda_r r_e + \psi_e + \boldsymbol{f}_r^{\mathrm{T}}\boldsymbol{\chi}_r(\boldsymbol{v}) - \dot{r}_d + \hat{F}_r - k_{r0}\chi_r\right) \tag{26}$$

where $\{\lambda_u, \lambda_r, k_{u0}, k_{r0}\} > 0$.

To analyze the influence of control input saturation on the system, the following auxiliary systems are designed.

$$\dot{\chi}_u = -k_{\chi u}\chi_u - \frac{|u_e\Delta\tau_u| + 0.5\rho_u^2\Delta\tau_u^2}{\chi_u}h(\chi_u) + \rho_u\Delta\tau_u \tag{27}$$

$$\dot{\chi}_r = -k_{\chi r}\chi_r - \frac{|r_e\Delta\tau_r| + 0.5\rho_r^2\Delta\tau_r^2}{\chi_r}h(\chi_r) + \rho_r\Delta\tau_r \tag{28}$$

where $h(\chi_i) = \begin{cases} 0, & |\chi_i| \leqslant \chi_a \\ 1 - \cos\left(\dfrac{\pi}{2}\sin\left(\dfrac{\pi}{2}\dfrac{\chi_i^2 - \chi_a^2}{\chi_b^2 - \chi_a^2}\right)\right), & \chi_a < |\chi_i| < \chi_b \\ 1, & |\chi_i| \geqslant \chi_b \end{cases}$

where $i = u, r$; $\{k_{\chi u}, \rho_u, k_{\chi r}, \rho_r\} > 0$, $\Delta\tau_r = \tau_r - \tau_{r0}$; $\Delta\tau_u = \tau_u - \tau_{u0}$; χ_a and χ_b are positive constants, and $\chi_b > \chi_a$.

The adaptive law of the lumped uncertainty is designed as

$$\begin{cases} \dot{\hat{F}}_u = \xi_u\left(\dfrac{u_e}{h_u} - \vartheta_u\hat{F}_u\right) \\ \dot{\hat{F}}_r = \xi_r\left(\dfrac{r_e}{h_r} - \vartheta_r\hat{F}_r\right) \end{cases} \tag{29}$$

where $\{\xi_u, \xi_r, \vartheta_u, \vartheta_r\} > 0$.

4 Stability analysis

1) Theorem. Eqs. (14)–(19) and Eqs. (25)–(29) are combined to make all signals of the guidance–control closed–loop system uniformly bounded. Moreover, the tracking error signal $\left(x - x_p, y - y_p, \psi - \psi_d\right)$ will converge to the sphere with the origin as the center of the sphere and a radius of m_{23}/m_{22}.

2) Proof. Lyapunov function is constructed as

$$V = V_1 + \frac{1}{2}\psi_e^2 + \frac{1}{2h_u}u_e^2 + \frac{1}{2h_r}r_e^2 + \frac{1}{2}\chi_u^2 + \frac{1}{2}\chi_r^2 + \frac{1}{2\xi_u}\tilde{F}_u^2 + \frac{1}{2\xi_r}\tilde{F}_r^2 \tag{30}$$

Taking the derivative of the function V with respect to time and combining Eqs. (22)–(29), we can get

$$\begin{aligned} \dot{V} = & -k_1 x_e^2 - k_y y_e^2 - k_\psi\psi_e^2 + \psi_e r_e + \\ & u_e\left(\frac{\boldsymbol{f}_u^{\mathrm{T}}\boldsymbol{\chi}_u(\boldsymbol{v})}{h_u} + \tau_u + \frac{F_u}{h_u} - \dot{u}_d\right) + \\ & r_e\left(\frac{\boldsymbol{f}_r^{\mathrm{T}}\boldsymbol{\chi}_r(\boldsymbol{v})}{h_r} + \tau_r + \frac{F_r}{h_r} - \dot{r}_d - \psi_e\right) - \tilde{F}_u\dot{\hat{F}}_u - \tilde{F}_r\dot{\hat{F}}_r + \\ & \chi_u\left(-k_{\chi u}\chi_u - \frac{|u_e\Delta\tau_u| + 0.5\rho_u^2\Delta\tau_u^2}{\chi_u}h(\chi_u) + \rho_u\Delta\tau_u\right) + \\ & \chi_r\left(-k_{\chi r}\chi_r - \frac{|u_e\Delta\tau_r| + 0.5\rho_r^2\Delta\tau_r^2}{\chi_r}h(\chi_r) + \rho_r\Delta\tau_r\right) \end{aligned} \tag{31}$$

After simplification, there is

$$\begin{aligned} \dot{V} = & -k_1 x_e^2 - k_y y_e^2 - k_\psi\psi_e^2 - \lambda_u u_e^2 - \lambda_r r_e^2 - k_{\chi u}\chi_u^2 - \\ & k_{\chi r}\chi_r^2 + k_{u0}u_e\chi_u + \vartheta_u\tilde{F}_u\hat{F}_u + k_{r0}r_e\chi_r + \\ & \vartheta_r\tilde{F}_r\hat{F}_r - |u_e\Delta\tau_u|\left[h(\chi_u) - \mathrm{sgn}(u_e\Delta\tau_u)\right] - \\ & 0.5\rho_u^2\Delta\tau_u^2 h(\chi_u) + \rho_u\Delta\tau_u\chi_u - 0.5\rho_r^2\Delta\tau_r^2 h(\chi_r) + \\ & \rho_r\Delta\tau_r\chi_r - |r_e\Delta\tau_r|\left[h(\chi_r) - \mathrm{sgn}(r_e\Delta\tau_r)\right] \end{aligned} \tag{32}$$

According to Cauchy inequality, there is

$$\begin{cases} k_{u0}u_e\chi_u \leqslant \dfrac{k_{u0}^2}{2}u_e^2 + \dfrac{1}{2}\chi_u^2; & \tilde{F}_u\hat{F}_u \leqslant -\dfrac{1}{2}\tilde{F}_u^2 + \dfrac{1}{2}F_{u\max}^2 \\ k_{r0}r_e\chi_r \leqslant \dfrac{k_{r0}^2}{2}r_e^2 + \dfrac{1}{2}\chi_r^2; & \tilde{F}_r\hat{F}_r \leqslant -\dfrac{1}{2}\tilde{F}_r^2 + \dfrac{1}{2}F_{r\max}^2 \\ \rho_u\Delta\tau_u\chi_u \leqslant \dfrac{1}{2}\rho_u^2\Delta\tau_u^2 + \dfrac{1}{2}\chi_u^2; & \rho_r\Delta\tau_r\chi_r \leqslant \dfrac{1}{2}\rho_r^2\Delta\tau_r^2 + \dfrac{1}{2}\chi_r^2 \end{cases} \tag{33}$$

Substituting Eq. (33) into Eq. (32), we can achieve

$$\dot{V}\leqslant -k_1x_{\mathrm{e}}^2-k_y y_{\mathrm{e}}^2-k_\psi\psi_{\mathrm{e}}^2-\left(\lambda_u-\frac{k_{u0}^2}{2}\right)u_{\mathrm{e}}^2-\left(\lambda_r-\frac{k_{r0}^2}{2}\right)r_{\mathrm{e}}^2-(k_{\chi u}-1)\chi_u^2-(k_{\chi r}-1)\chi_r^2-|u_{\mathrm{e}}\Delta\tau_u|\left[h(\chi_u)-\mathrm{sgn}(u_{\mathrm{e}}\Delta\tau_u)\right]-|r_{\mathrm{e}}\Delta\tau_r|\left[h(\chi_r)-\mathrm{sgn}(r_{\mathrm{e}}\Delta\tau_r)\right]-\left(\frac{h(\chi_u)}{2}-\frac{1}{2}\right)\rho_u^2\Delta\tau_u^2-\left(\frac{h(\chi_r)}{2}-\frac{1}{2}\right)\rho_r^2\Delta\tau_r^2-\frac{\vartheta_u}{2}\tilde{F}_u^2-\frac{\vartheta_r}{2}\tilde{F}_r^2+\frac{\vartheta_u}{2}F_{u\max}^2+\frac{\vartheta_r}{2}F_{r\max}^2 \tag{34}$$

When $h(\chi_u)=h(\chi_r)=1$, there is

$$\dot{V}\leqslant -k_1x_{\mathrm{e}}^2-k_y y_{\mathrm{e}}^2-k_\psi\psi_{\mathrm{e}}^2-\left(\lambda_u-\frac{k_{u0}^2}{2}\right)u_{\mathrm{e}}^2-\left(\lambda_r-\frac{k_{r0}^2}{2}\right)r_{\mathrm{e}}^2-(k_{\chi u}-1)\chi_u^2-(k_{\chi r}-1)\chi_r^2-\frac{\vartheta_u}{2}\tilde{F}_u^2-\frac{\vartheta_r}{2}\tilde{F}_r^2+\frac{\vartheta_u}{2}F_{u\max}^2+\frac{\vartheta_r}{2}F_{r\max}^2\leqslant -2k_{v1}V+\Xi_{v1} \tag{35}$$

where $k_{v1}=\min\left\{k_1,k_y,k_\psi,\lambda_u-\frac{k_{u0}^2}{2},\lambda_r-\frac{k_{r0}^2}{2},k_{\chi u}-1,k_{\chi r}-1,\frac{\vartheta_u}{2},\frac{\vartheta_r}{2}\right\}$; $\Xi_{v1}=\frac{\vartheta_u}{2}F_{u\max}^2+\frac{\vartheta_r}{2}F_{r\max}^2$.

When $h(\chi_u)<1$ and $h(\chi_r)<1$, according to $u_{\mathrm{e}}\Delta\tau_u\leqslant\frac{1}{2}u_{\mathrm{e}}^2+\frac{1}{2}\Delta\tau_u^2$ and $r_{\mathrm{e}}\Delta\tau_r\leqslant\frac{1}{2}r_{\mathrm{e}}^2+\frac{1}{2}\Delta\tau_r^2$, we can obtain

$$\dot{V}\leqslant -k_1x_{\mathrm{e}}^2-k_y y_{\mathrm{e}}^2-k_\psi\psi_{\mathrm{e}}^2-\left(\lambda_u-\frac{k_{u0}^2-1}{2}\right)u_{\mathrm{e}}^2-\left(\lambda_r-\frac{k_{r0}^2-1}{2}\right)r_{\mathrm{e}}^2-(k_{\chi u}-1)\chi_u^2-(k_{\chi r}-1)\chi_r^2-\frac{\vartheta_u}{2}\tilde{F}_u^2-\frac{\vartheta_r}{2}\tilde{F}_r^2+\left(\frac{\rho_u^2}{2}+\frac{1}{2}\right)\Delta\tau_u^2+\left(\frac{\rho_r^2}{2}+\frac{1}{2}\right)\Delta\tau_r^2+\frac{\vartheta_u}{2}F_{u\max}^2+\frac{\vartheta_r}{2}F_{r\max}^2\leqslant -k_{v2}V+\Xi_{v2} \tag{36}$$

where $k_{v2}=\min\left\{k_1,k_y,k_\psi,\lambda_u-\frac{k_{u0}^2-1}{2},\lambda_r-\frac{k_{r0}^2-1}{2},k_{\chi u}-1,k_{\chi r}-1,\frac{\vartheta_u}{2},\frac{\vartheta_r}{2}\right\}$; $\Xi_{v2}=\left(\frac{\rho_u^2}{2}+\frac{1}{2}\right)\Delta\tau_u^2+\left(\frac{\rho_r^2}{2}+\frac{1}{2}\right)\Delta\tau_r^2+\frac{\vartheta_u}{2}F_{u\max}^2+\frac{\vartheta_r}{2}F_{r\max}^2$. Combining Eq. (35) with Eq. (36), we can obtain

$$\dot{V}\leqslant -2k_vV+\Xi_v \tag{37}$$

where $k_v=\min\{k_{v1},k_{v2}\}$; $\Xi_v=\max\{\Xi_{v1},\Xi_{v2}\}$. The design parameters satisfy $\lambda_u>\frac{k_{u0}^2}{2},\lambda_r>\frac{k_{r0}^2}{2},k_{\chi u}>1,k_{\chi r}>1$. According to Eq. (37), it can be found that

$$V\leqslant\left(V(0)-\frac{\Xi_v}{2k_v}\right)\mathrm{e}^{-k_vt}+\frac{\Xi_v}{2k_v} \tag{38}$$

Therefore, it can be concluded from the above equations that V is bounded, and the system error signals $x_{\mathrm{e}},y_{\mathrm{e}},\psi_{\mathrm{e}},u_{\mathrm{e}},r_{\mathrm{e}},\chi_u,\chi_r,\tilde{F}_u$ and $\tilde{F}_r$ are uniformly bounded and stable.

5 Numerical simulation

To verify the effectiveness of the proposed tracking control of the backstepping adaptive path based on the surge-varying LOS, two groups of comparative experiments are taken on USV dynamic model Eq. (3) and Eq. (23) (Fig. 2-Fig. 6). Considering the input saturation, the simulation results of the improved surge-varying LOS and LOS without surge-varying (traditional LOS) are compared in the first group. The longitudinal velocity is set to the constant velocity of 0.1 m/s during the stable sailing. In the second group, the simulation results of the cases considering and not considering the input saturation are compared. Parameters of USV are shown in Reference [17]. The maximum value of longitudinal control input is set as 4 N, and the maximum control moment of yawing is 0.3 N·m.

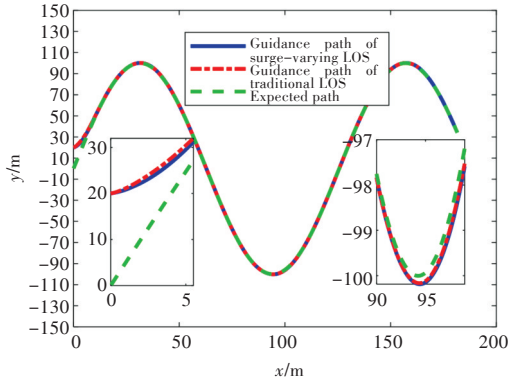

(a) The first group of comparative experiments

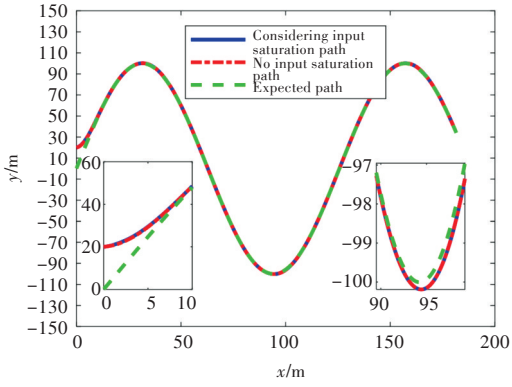

(b) The second group of comparative experiments

Fig.2 Performance comparison of the path following

The initial state of the USV is $[x(0)\ y(0)\ \psi(0)]^{\mathrm{T}}=[0\ 20\ \pi/7]^{\mathrm{T}}$, $[u(0)\ v(0)\ r(0)]^{\mathrm{T}}=[0\ 0\ 0]^{\mathrm{T}}$.

The design parameters of the controller are $k=1,k_1=0.5,k_\psi=0.1,\lambda_u=3,\lambda_r=1,\chi_a=0.01,\chi_b=$

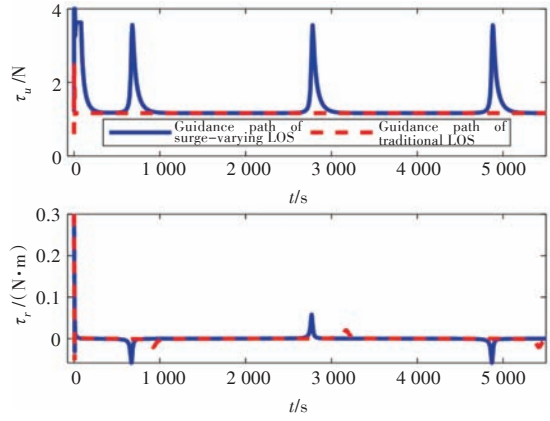

(a) The first group of comparative experiments

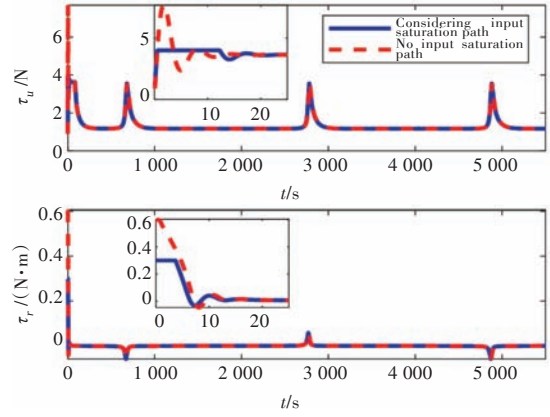

(b) The second group of comparative experiments

Fig.3 Comparison of different control inputs

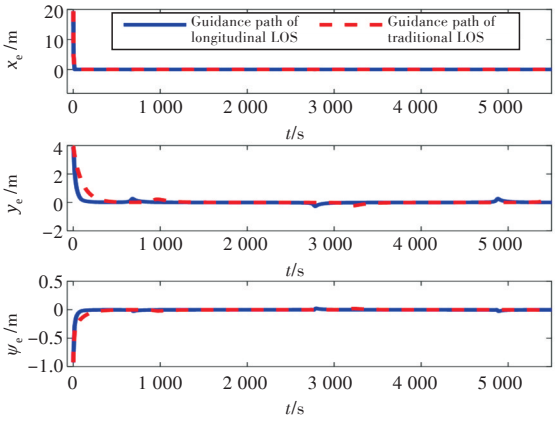

(a) The first group of comparative experiments

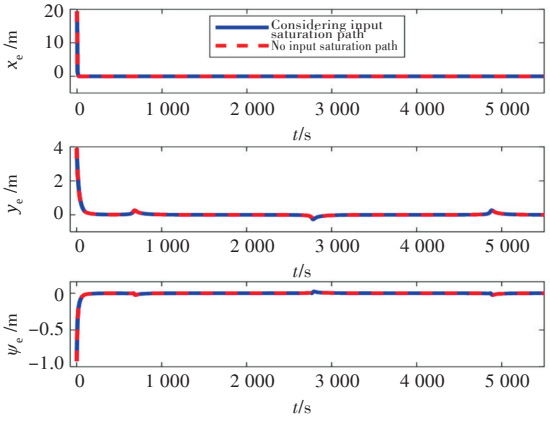

(b) The second group of comparative experiments

Fig.4 The errors of position and heading

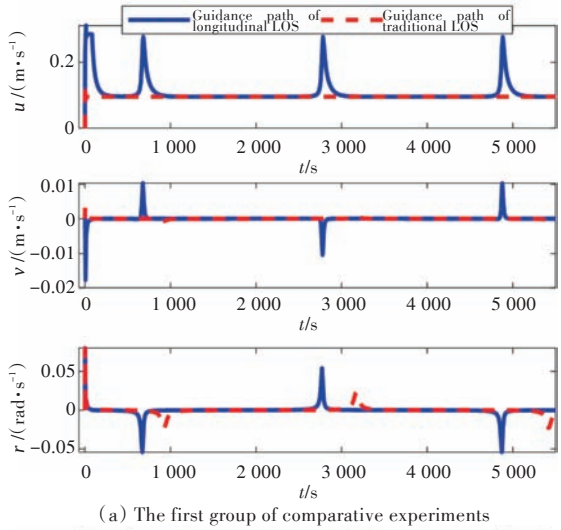

(a) The first group of comparative experiments

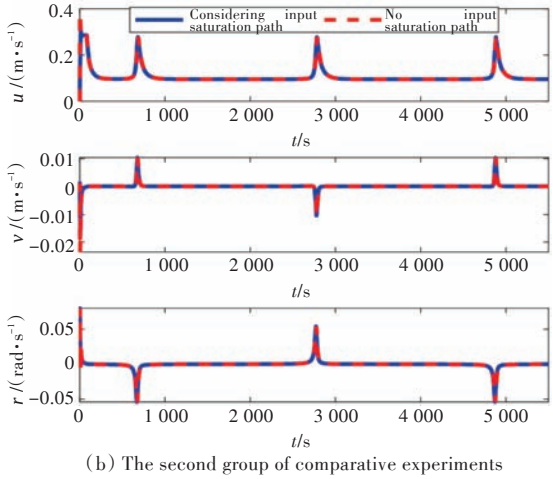

(b) The second group of comparative experiments

Fig.5 The state comparison of system velocity

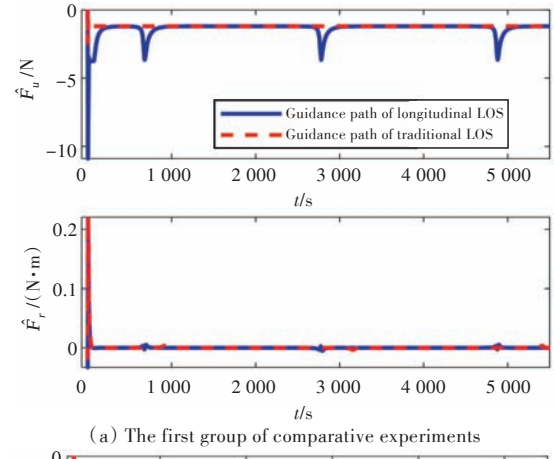

(a) The first group of comparative experiments

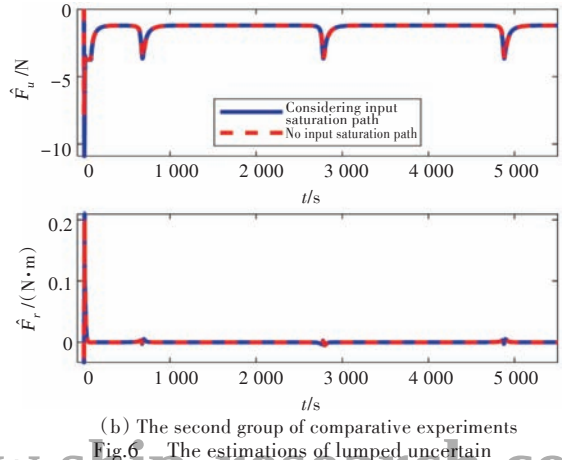

(b) The second group of comparative experiments

Fig.6 The estimations of lumped uncertain

$0.1, k_{\chi u}=2,\ k_{\chi r}=2,\ \rho_u=1, \rho_r=1, k_{u0}=0.01, k_{r0}=0.1, \vartheta_u=0.1, \vartheta_r=0.1, u_{\max}=0.3$.

The expected sinusoidal reference path is $x_p(\theta)=\theta, y_p(\theta)=100\theta\sin(0.05\theta)$.

From the simulation results, the surge-varying LOS is better than the traditional LOS, and it has a faster convergence velocity and better transient and steady-state tracking performance [Fig. 2 (a)]. Simultaneously, the simulation results of the second group show that the desired path tracking performance of controller can be achieved with the control input saturation considered or not. However, with considering it, the controller can satisfy the system input saturation limit and has better tracking performance [Fig. 2 (b)]. From Fig. 3 (a), when the expected path curvature is large, the transverse error of surge-varying LOS increases. Thus, accelerating of longitudinal velocity leads to the increase in the longitudinal control input, and thus achieving a better tracking effect. When the input saturation is taken into consideration, the system can still achieve a good tracking performance. While without considering it, the control input of system significantly exceeds the maximum of actuators, which will lead to difficulties in achieving an effective tracking performance (Fig. 3) for the actual system. In Fig. 4 (a), compared with the traditional LOS, the surge-varying LOS has a faster convergence speed and thus the tracking speed of the whole system is increased. In Fig. 5, the change trends of system velocity state in the process of path tracking are compared, and it is found that due to the large horizontal position error in the early stage, the longitudinal velocity is high. As the position error decreases, the system speed stabilizes in a constant value related to the forward distance Δ. Fig. 6 is the estimate of a mixed unknown item, where $\hat{F}_u$ is close to 0, and $\hat{F}_r$ eventually approaches zero because the yawing error finally converges to zero.

6 Conclusions

The control method of backstepping adaptive path based on the surge-varying LOS proposed in this paper solves the lumped uncertainties of USV and the path tracking problem of system inertial matrix with non-zero non-diagonal terms and controller input saturation. The coordinate transformation is introduced to transform the system model into the skew-symmetric form, which simplifies the design of the controller. In the guidance subsystem, the guidance law of surge-varying LOS is developed to ensure that USV can effectively go towards and keep on the expected path and make guidance law of longitudinal speed positively correlated to the transverse tracking error. Therefore, the convergence time of system error is reduced and the robustness of the system is enhanced. In the control subsystem, the lumped uncertainties and the problem caused by the saturation of control input of system are solved by constructing the backstepping adaptive method and the auxiliary system, which makes USV reach the desired path tracking performance. According to Lyapunov stability theories, the guidance-control closed-loop system is proved to be uniformly bounded. The simulation results verify that the proposed method can effectively track the expected path, meet the system characteristics of dynamic and actuator saturation, and have robustness on the system modeling error and parameter perturbation. The problem of interference on the skew-symmetric model system compensated by the observer will be further researched.

References

[1] Zheng Z W, Feroskhan M. Path following of a surface vessel with prescribed performance in the presence of input saturation and external disturbances [J]. IEEE/ASME Transactions on Mechatronics, 2017, 22(6): 2564-2575.

[2] Liu L, Wang D, Peng Z H. Path following of marine surface vehicles with dynamical uncertainty and time-varying ocean disturbances [J]. Neurocomputing, 2016, 173: 799-808.

[3] Wang N, Sun Z, Su S F, et al. Fuzzy uncertainty observer-based path-following control of underactuated marine vehicles with unmodeled dynamics and disturbances [J]. International Journal of Fuzzy Systems, 2018, 20(8): 2593-2604.

[4] Zhang G Q, Zhang X K, Zheng Y F. Adaptive neural path-following control for underactuated ships in fields of marine practice [J]. Ocean Engineering, 2015, 104: 558-567.

[5] Fossen T I. Handbook of marine craft hydrodynamics and Motion Control [M]. United Kingdom: Wiley, 2011.

[6] Guo C, Wang Y, Sun F C, et al. Survey for motion control of underactuated surface vessels [J]. Control and Decision, 2009, 24(3): 321-329 (in Chinese).

[7] Liu Y. The nonlinear adaptive control for underactuated surface vessels [D]. Dalian: Dalian Maritime University, 2010 (in Chinese).

[8] Wang N, Sun Z, Yin J C, et al. Finite-time observer based guidance and control of underactuated surface vehicles with unknown sideslip angles and disturbances

[J]. IEEE Access, 2018, 6: 14059-14070.

[9] Zheng Z W, Sun L, Xie L H. Error-constrained LOS path following of a surface vessel with actuator saturation and faults [J]. IEEE Transactions on Systems, Man, and Cybernetics: Systems, 2018, 48 (10): 1794-1805.

[10] Miao J M, Wang S P, Tomovic M M, et al. Compound line-of-sight nonlinear path following control of underactuated marine vehicles exposed to wind, waves, and ocean currents [J]. Nonlinear Dynamics, 2017, 89(4): 2441-2459.

[11] Liu L, Wang D, Peng Z H. ESO-based line-of-sight guidance law for path following of underactuated marine surface vehicles with exact sideslip compensation [J]. IEEE Journal of Oceanic Engineering, 2017, 42 (2): 477-487.

[12] Fossen T I, Pettersen K Y, Galeazzi R. Line-of-sight path following for Dubins paths with adaptive sideslip compensation of drift forces [J]. IEEE Transactions on Control Systems Technology, 2015, 23 (2): 820-827.

[13] Lekkas A M, Fossen T I. Integral LOS path following for curved paths based on a monotone cubic Hermite spline parametrization [J]. IEEE Transactions on Control Systems Technology, 2014, 22(6): 2287-2301.

[14] Liu T, Dong Z P, Du H W, et al. Path following control of the underactuated USV based on the improved line-of-sight guidance algorithm [J]. Polish Maritime Research, 2017, 24(1): 3-11.

[15] Dong Z P, Wan L, Liao Y L, et al. Path following control of underactuated USV based on asymmetric model [J]. Shipbuilding of China, 2016, 57 (1): 116-126 (in Chinese).

[16] Shi Y, Shen C, Fang H Z, et al. Advanced control in marine mechatronic systems: a survey [J]. IEEE/ASME Transactions on Mechatronics, 2017, 22(3): 1121-1131.

[17] Do K D, Pan J. Underactuated ships follow smooth paths with Integral actions and without velocity measurements for feedback: theory and experiments [J]. IEEE Transactions on Control Systems Technology, 2006, 14(2): 308-322.

[18] Shen H Q, Guo C. Path-following control of underactuated ships using actor-critic reinforcement learning with MLP neural networks [C]//Proceedings of the 2016 6th International Conference on Information Science and Technology. Dalian, China: IEEE, 2016.

[19] Yan Z P, Duan H P. A double closed-loop Terminal sliding mode controller for the trajectory tracking of UUV [J]. Chinese Journal of Ship Research, 2015, 10(4): 112-117, 142 (in Chinese).

[20] Cao S J, Zeng F M, Chen Y T. The course and speed cooperative control method for unmanned surface vehicles [J]. Chinese Journal of Ship Research, 2015, 10(6): 74-80 (in Chinese).

[21] Li T S, Li R H, Li J F. Decentralized adaptive neural control of nonlinear interconnected large-scale systems with unknown time delays and input saturation [J]. Neurocomputing, 2011, 74(14/15): 2277-2283.

[22] Liu C, Chen C L P, Zou Z J, et al. Adaptive NN-DSC control design for path following of underactuated surface vessels with input saturation [J]. Neurocomputing, 2017, 267: 466-474.

[23] Yu H M. Research on trajectory tracking control for underactuated UUV with nonlinear constrained factors [D]. Harbin: Harbin Engineering University, 2016 (in Chinese).

[24] Do K D, Pan J. Global tracking control of underactuated ships with nonzero off-diagonal terms in their system matrices [J]. Automatica, 2005, 41 (1): 87-95.

[25] Ma B L, Xie W J. Global asymptotic trajectory tracking and point stabilization of asymmetric underactuated ships with non-diagonal inertia/damping matrices [J]. International Journal of Advanced Robotic Systems, 2013, 10(9): 336.

基于速变LOS的无人船反步自适应路径跟踪控制

余亚磊[1], 苏荣彬[1], 冯旭[1], 郭晨[*2]

1 大连海事大学 航海学院,辽宁 大连 116026

2 大连海事大学 船舶电气工程学院,辽宁 大连 116026

摘　要:[**目的**]为了解决无人船由系统建模误差和参数摄动引起的混合不确定项、模型含非零非对角项和控制器输入饱和情况下的路径跟踪问题,[**方法**]提出基于速变视线导航法(LOS)的反步自适应无人船路径跟踪控制方法。首先引入坐标变换法,把系统模型转变为斜对角形式。把控制系统分为制导子系统和控制子系统,在制导子系统设计速变LOS算法,使纵向速度制导律与横向跟踪误差呈正相关,确保无人船能有效地朝着并保持在期望的路径上;在控制子系统设计反步自适应算法以补偿系统混合不确定项,同时引入辅助系统处理系统控制输入饱和问题。[**结果**]运用李雅普诺夫稳定性理论证明制导—控制闭环系统一致最终有界稳定。[**结论**]仿真结果验证了所提出方法的有效性和鲁棒性,对无人船反步自适应路径跟踪控制有一定的参考价值。

关键词:无人船; 路径跟踪; 视线导航法; 输入饱和; 自适应控制